SCIENCE CHINA
Physics, Mechanics & Astronomy

• Research Paper •
Hydrodynamics in Ocean Engineering

January 2011 Vol.54 No.1: 16–25
doi: 10.1007/s11433-010-4194-8

# Modelling of multi-bodies in close proximity under water waves —Fluid resonance in narrow gaps

LU Lin[1,2*], TENG Bin[3*], CHENG Liang[4], SUN Liang[5] & CHEN XiaoBo[6]

[1] *Center for Deepwater Engineering, Dalian University of Technology, Dalian 116024, China;*
[2] *State Key Laboratory of Structural Analysis for Industrial Equipment, Dalian University of Technology, Dalian 116024, China;*
[3] *State Key Laboratory of Coastal and Offshore Engineering, Dalian University of Technology, Dalian 116024, China;*
[4] *School of Civil and Resource Engineering, The University of Western Australia, Crawly 6003, Australia;*
[5] *Centre for Offshore Research and Engineering, Department of Civil Engineering, National University of Singapore, 117576, Singapore;*
[6] *Research Department, Bureau Veritas, Neuilly-Sur-Seine, 92570, France*

Received June 28, 2010; accepted July 26, 2010; published online November 29, 2010

Viscous fluid model and potential flow model with and without artificial damping force ($f = -\mu V$, $\mu$ the damping coefficient and $V$ the local averaging flow velocity) are employed in this work to investigate the phenomenon of fluid resonance in narrow gaps between multi-bodies in close proximity under water waves. The numerical results are compared with experimental data available in the literature. The comparison demonstrates that both the viscous fluid model and the potential flow model are able to predict the resonant frequency reasonably well. However the conventional potential flow model (without artificial damping term) significantly over-predicts the wave height in narrow gaps around the resonant frequency. In order to calibrate the appropriate damping coefficient used for the potential model and make it work as well as the viscous fluid model in predicting the resonant wave height in narrow gaps but with little computational efforts, the dependence of damping coefficient $\mu$ on the body geometric dimensions is examined considering the parameters of gap width $B_g$, body draft $D$, body breadth ratio $B_r$ and body number $n$ ($n$ = 2, 3), where $B_r = B_B/B_A$ for the case of two bodies (Body A and Body B) with different breadths of $B_A$ and $B_B$, respectively. It was confirmed that the damping coefficient used for the potential flow model is not sensitive to the geometric dimensions and spatial arrangement. It was found that $\mu \in [0.4, 0.5]$ may guarantee the variation of $H_g/H_0$ with $kh$ to be generally in good agreement with the experimental data and the results of viscous fluid model, where $H_g$ is the excited wave height in narrow gaps under various dimensionless incident wave frequencies $kh$, $H_0$ is the incident wave height, $k = 2\pi/L$ is the wave number and $h$ is the water depth.

**narrow gap, fluid resonance, water wave, viscous fluid model, potential flow model, finite element method, boundary element method**

**PACS:** 47.35.Lf, 47.10.ad, 47.15.km, 47.85.Dh, 47.11.Fg, 47.11.Hj

Multiple floating structures arranged side by side with small separations are often encountered in marine and offshore practices, such as the Very Large Floating Structure (VLFS) involving many separated modules [1], side-by-side operations between a Liquefied Natural Gas (LNG) tank and a Floating Production Storage and Offloading facility (FPSO) [2] and a large vessel berthing in front of wharf [3,4]. The characteristic dimensions of the gaps between the neighboring structures are usually very small in comparison with the dimensions of the structures. When the multi-floating structures with narrow gaps are subjected to water waves, fluid resonance may take place, which can lead to the vertical oscillations of the mean surface with amplitudes substantially larger than the incident wave in the narrow gaps and the increase of wave forces on the structures

*Corresponding author (email: LuLin@dlut.edu.cn; BTeng@dlut.edu.cn)

around the resonant frequencies. The resonant wave frequency, wave height and wave forces are of engineering significance. Many efforts have been devoted to these aspects, for example, the model tests [5,6], theoretical analysis [7,8] and numerical investigations [9–13], among others.

The early experimental examinations associated with the present concerned fluid resonance may be initialed in the problem of sloshing resonance in moon pool of FPSO, where the considerable piston-mode motions were paid much more attention in addition to the sloshing-mode [14,15]. As for the narrow gaps formed by multi-structure in close approximation, the sloshing mode may be ignored. This allows therefore the investigations to be conducted in a simplified two-dimensional space, which is particularly desirable under the conditions that the wave traveling direction is normal to the narrow gap. Focusing on this situation, both Saitoh et al. [5] and Iwata et al. [6] conducted experimental investigations in virtue of laboratory facility of wave flume. They measured the wave height in narrow gaps under various incident wave numbers for twin boxes with single narrow gap and three identical boxes with double narrow gaps, respectively. Their experimental results indicate that the maximal amplitude of resonant wave motion excited in narrow gaps may even approach up to about five times of the incident wave amplitude. Also, it was confirmed that the resonant frequency and the corresponding resonant wave height are correlated closely to the box draft, the gap width and the number of boxes.

On the other hand, numerical examinations are also carried out during the last two decades. The numerical models developed so far are mainly within the framework of potential flow theory, such as those based on boundary integral method [9,16,17] and scaled boundary finite element method [10,12,13] in frequency domain and the boundary element based three-dimensional model in time domain [18]. It was understood that the conventional potential flow model tends to over-predict the wave amplitudes in the narrow gaps because the physical energy dissipations due to fluid viscosity, vortex shedding and even turbulence can not be taken into account in the context of potential flow theory.

Attempts have been made to introduce some amount of resistance artificially in order to overcome the difficulties from conventional potential flow model, such as the rigid lid [19], linear damping term as body force [20], and linear dissipative term in free surface boundary condition [21–23]. Particularly, the vortex method was also employed to simulate the fluid resonance in narrow gaps and reasonable results were obtained [3,4]. It has been shown that the technique by incorporating artificial resistance into the conventional potential flow model may work well in limiting the amplitude of water oscillations in narrow gaps, at least for some special situations. However, the specification of the magnitude of artificial resistance remains uncertain if the structure geometric dimensions and operational arrangement are changed.

As mentioned previously, the real-life fluid viscosity and energy dissipation has to be considered seriously if the accurate prediction on fluid resonance in narrow gaps is required. A straightforward manner to develop such a numerical model is to adopt the fundamental Navier-Stokes equations to describe the actual viscous fluid flow. However, the performance of the viscous fluid model equipped with free surface capture technique to simulate violent wave oscillation in narrow gaps are shown to be very time-consuming although it is able to produce indeed the satisfying numerical results as expected [24–26]. The main purpose of this work is to investigate the problem of fluid resonance in narrow gaps using both the viscous fluid model and the potential flow model. Based on comprehensive numerical validations and comparisons, the damping coefficient for potential flow model is calibrated considering various geometric characteristics and arrangements of the floating bodies. Such that the extreme large wave oscillation under resonance in the narrow gaps formed by multi-body can be predicted reasonably in the frame of the potential flow theory with high computational efficiency.

## 1 Numerical model

### 1.1 Viscous fluid model

The viscous numerical model used in this work consists of a three-step finite element [27] solver for Navier-stokes equations, an internal wave maker [28] for wave generation, a CLEAR Volume of Fluid (CLEAR-VOF) technique [29] for free surface capture and a spongy layer for reducing undesirable reflected waves.

The conservation laws of mass and momentum for incompressible viscous Newtonian fluids are governed by the Navier-Stokes equations,

$$\frac{\partial u_i}{\partial x_i} = \begin{cases} q(\boldsymbol{x},t), & \boldsymbol{x} \in \Omega_s, \\ 0, & \boldsymbol{x} \notin \Omega_s, \end{cases} \tag{1}$$

$$\frac{\partial u_i}{\partial t} + u_j \frac{\partial u_i}{\partial x_j} = -\frac{1}{\rho}\frac{\partial p}{\partial x_i} + \upsilon \frac{\partial}{\partial x_j}\left(\frac{\partial u_i}{\partial x_j}\right) + f_i + \frac{\upsilon}{3}\frac{\partial q}{\partial x_i}, \tag{2}$$

where $u_i$ and $f_i$ are the velocity and body forces components in the $i$ direction and $p$, $\rho$, $v$ denote the pressure, fluid density and kinematic viscosity, respectively. It should be pointed out that no turbulent model is included in the present viscous numerical wave flume. Alternatively, the turbulence is accounted for by the direct numerical simulation in the two dimensional space with very fine meshes. In eq. (1), a source term $q(\boldsymbol{x}, t)$ is used in the source region $\Omega_s$ to generate desirable incident waves by means of the method of internal wave maker [28]. Considering the linear monochromatic wave used in this work, the source function reads:

$$q(t) = CH_0 \sin(\omega t)/S, \tag{3}$$

where $C$ is the phase velocity of the target wave, $H_0$ is the incident wave height with $H_0 = 2A$ and $A$ is the wave amplitude, $\omega$ denotes the wave frequency with $\omega = 2\pi/T$, $T$ is the wave period and $S$ is the area of the source region. In order to save computational efforts, the reflected wave is reduced by means of spongy layers located at both ends of the computational domain. This is implemented numerically by introducing additional damping force into the body force term of Navier-Stokes equation:

$$f_i = g_i + R_i, \tag{4}$$

where $f_i$ denotes the external force in the $x_i$ direction, $g_i$ is the gravitational force and $R_i$ is the damping force used in spongy layer [30]:

$$R_y = -k_s \left( \frac{x - x_0}{D_s} \right)^2 \frac{y_b - y}{y_b - y_h} \cdot u_y, \tag{5}$$

where $x$ and $y$ are the Cartesian coordinates of grid nodes, $x_0$ is the coordinate at the start points of spongy layers, $D_s$ is the total length of damping zone in the direction of wave propagation, $y_b$ is the elevation of seabed, $y_h$ is the local maximum elevation of the free surface and $k_s$ is an empirical parameter determined by some trivial numerical tests beforehand. For the sake of numerical stability, the damping term is only activated in the vertical direction, that is, $R_x = 0$.

The governing equations are discretized in time and space using the upwind three-step Taylor-Galerkin finite element method [27]. Owing to the projection procedure involved in the present numerical discritization, the velocity and pressure can be decoupled and solved separately. In this work, the velocities are solved by means of mass lumped technique [31], while the BI-CGSTAB method [32] is adopted to obtain pressure.

The Computational Lagrangian-Eulerian Advection Remap Volume of Fluid method [29] is used to capture the violent free surface. Different from the usual VOF method, the fluid advection in CLEAR-VOF is implemented by moving a 'fluid polygon' in a Lagrangian sense which allows the CLEAR-VOF to be inherently consistent with the finite element method and irregular mesh partition. For the present water wave problem, the inertia influence of air phase is neglected but without the loss of compromising computational accuracy. Consequently, the void cells are not considered during the numerical simulations and the full elements are dealt with the usual manner in the finite element method, whereas the partial elements are treated specially by means of averaging the density and viscosity

$$\rho = \varphi\rho_w + (1-\varphi)\rho_a, \quad \upsilon = \varphi\upsilon_w + (1-\varphi)\upsilon_a, \tag{6}$$

where the subscripts $w$ and $a$ represent water and air, respectively.

The numerical computations start from still water, which means the initial velocity condition is $\boldsymbol{u}(\boldsymbol{x}, 0) = 0$ and the static water pressure is applied. At the ends of sponge layers, the bottom of numerical wave flume and the solid walls of the floating bodies, the non-slip boundary condition is imposed. According to the requirements of stress balance, both pressure and velocity boundary conditions need to be treated at the free surface. By neglecting the viscous effects a simple normal dynamic free surface boundary condition $p = 0$ is implemented. While the widely used velocity extrapolations [33,34] are incorporated in the present viscous numerical wave flume. The mesh resolution and time step dependence associated with the present viscous numerical model has been verified carefully in our previous work [24–26]. In general, the total number of meshes used in this work are generally more than 100000 with the smallest grid size of $B_g/20 \times B_g/20$ in the narrow gaps, where $B_g$ is the gap width. The time step is automatically determined in the program using the uniform CFL condition multiplied by a safe factor of 0.2.

### 1.2 Potential flow model

The conventional potential flow model is based on the assumptions that the fluid flow is incompressible, inviscid and irrotational. The two-dimensional mass conservation of potential flow is commonly written in the form of Laplace Equation:

$$\frac{\partial^2 \Phi(x, y, t)}{\partial x^2} + \frac{\partial^2 \Phi(x, y, t)}{\partial y^2} = 0, \tag{7}$$

where $\Phi(x, y, t)$ is the well-known velocity potential. For harmonic wave motion, the time dependent part can be separated out as $\Phi(x, y, t) = \mathrm{Re}[\phi(x, y)\mathrm{e}^{-\mathrm{i}\omega t}]$, where $\phi(x, y)$ is the complex potential. For simplicity, $\phi(x, y)$ is divided into the incident potential and the scattering potential, that is

$$\phi(x, y) = \phi_I(x, y) + \phi_S(x, y). \tag{8}$$

As for the linear water wave, the incident potential $\phi_I(x, y)$ reads

$$\phi_I(x, y) = -\frac{\mathrm{i}gA}{\omega \cosh kh} \cosh k(y + h)\mathrm{e}^{\mathrm{i}kx}, \tag{9}$$

in which, $g$ is the gravitational acceleration, $A = H_0/2$ is the incident wave amplitude and $H_0$ is the incident wave height, $\omega = 2\pi/T$ is the wave angular frequency and $T$ is the wave period, $k = 2\pi/L$ is the wave number and $L$ is the wave length, $h$ is the water depth.

In order to model the flow resistance in the narrow gaps within the frame of potential flow theory, a damping term is introduced in the momentum equation [21–23]:

$$f = -\mu(x)V = -\mu(x)\nabla\Phi, \tag{10}$$

where $\mu$ is an artificial damping coefficient and $V$ is the averaging flow velocity in the narrow gaps. By using the first order approximation of wave profile $\zeta$, we have

$$\zeta(x,y,t) = -\frac{1}{g}\Phi_t(x,y,t) - \frac{\mu}{g}(x)\Phi(x,y,t). \tag{11}$$

Considering the kinematic condition on the free surface, $\partial\zeta/\partial t = \partial\Phi/\partial y$ , eq. (11) can be re-written as:

$$\frac{\partial\Phi^2(x,y,t)}{\partial t^2} + \mu(x)\frac{\partial\Phi(x,y,t)}{\partial t} = -g\frac{\partial\Phi(x,y,t)}{\partial y}. \tag{12}$$

Accordingly, the time-independent complex potential reads

$$\frac{\partial\phi}{\partial y} = \frac{1}{g}\left(\omega^2\phi + \mathrm{i}\omega\mu\,\phi\right). \tag{13}$$

The scattering potential satisfies the Laplace Equation as well and is subjected to the following boundary conditions: $\partial\phi_S/\partial y = \left(\omega^2\phi_S + \mathrm{i}\omega\mu\,\phi_S\right)/g$ at the free surface of $y$ = 0; $\partial\phi_S/\partial n = -\partial\phi_I/\partial n$ along the solid wall of structures; $\partial\phi_S/\partial y = 0$ at the sea bottom $y$ = –$h$; $\partial\phi_S/\partial x = -\mathrm{i}k\phi_S$ at the far field upstream and $\partial\phi_S/\partial x = \mathrm{i}k\phi_S$ at the downstream.

The above governing equations for potential flow together with the boundary conditions are solved using a boundary element method [35]. In the present potential flow model, only the first order results are concerned. The grid points used in this work are 2257, leading to 1128 mesh cells. The fine meshes are generated in the narrow gaps with 8 uniform cells, while the coarse meshes are used in the far field. The computational meshes have been confirmed to produce convergent solutions.

## 2 Numerical results

The previously described viscous numerical wave flume and the potential flow model with different artificial damping coefficients were employed to investigate the fluid resonance in the narrow gaps formed by rectangular boxes. The available laboratory test results by Saitoh et al. [5] and Iwata et al. [6] were adopted to validate the numerical results. In the laboratory tests, two or three identical boxes with the same breadth $B$ = 0.5 m are fixed in a wave flume with water depth $h$ = 0.5 m. Different drafts $D$ and gap width $B_g$ are considered in the experiments. The incident wave heights $H_0$ range from 0.023 m to 0.025 m in the laboratory tests. The input parameters of the numerical model are set up as closely as possible to those used in the experiments. A sketch definition of the numerical and experimental setup is illustrated in Figure 1.

We considered the influences from gap width $B_g$, body draft $D$, box breadth ratio $B_r$ and the number of bodies $n$. The numerical results from the potential flow model with different damping coefficients are compared with available experimental data and the viscous numerical results. For the special cases of two boxes with different breadths, the potential results are compared only with the viscous numerical results because of the absence of experimental data. By means of the comparisons, the appropriate damping coefficient for the multi-box assembly involving different structure configurations is determined.

### 2.1 Influence of gap width

We first considered the situations of twin bodies with single narrow gap. The two boxes are with the same breadth 0.5 m and draft 0.252 m as adopted in the experiments [5]. The influence of the gap width on the fluid resonance in narrow gap is investigated involving three typical gap widths of 0.03 m, 0.05 m and 0.07 m. The variations of averaging wave height $H_g/H_0$ in the narrow gap with respect to the non-dimensional wave number $kh$ are plotted in Figure 2. Note that the details of the free surface evolution can be found in our previous work [24–26] and are omitted in this article. For the purpose of comparison, the experimental data [5], the numerical results from viscous numerical wave flume and the potential flow model with different values of damping coefficients ($\mu$ = 0.0, 0.3, 0.4 and 0.5) are also included in this figure.

It appears that both the viscous fluid model and the potential flow model predict the resonant frequency accurately. The predicted resonant frequencies are very close to those observed in the laboratory tests. The variation of $H_g/H_0$ with $kh$ obtained using the viscous numerical model is seen to agree well with the experimental data. The relative errors of the maximum wave heights between the viscous fluid model and the experimental data are less than 10%. It should be noted that it is difficult to determine the resonant frequency and the corresponding resonant wave height in narrow gap with high accuracy using the viscous fluid model because the very small frequency increment is required to meet with the high resolution. This is not easy to implement as the potential flow model since the viscous fluid model is very time-consuming. Our numerical simulation experience

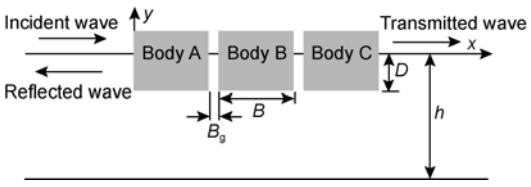


**Figure 1** Sketch definition of the numerical and experimental setup.

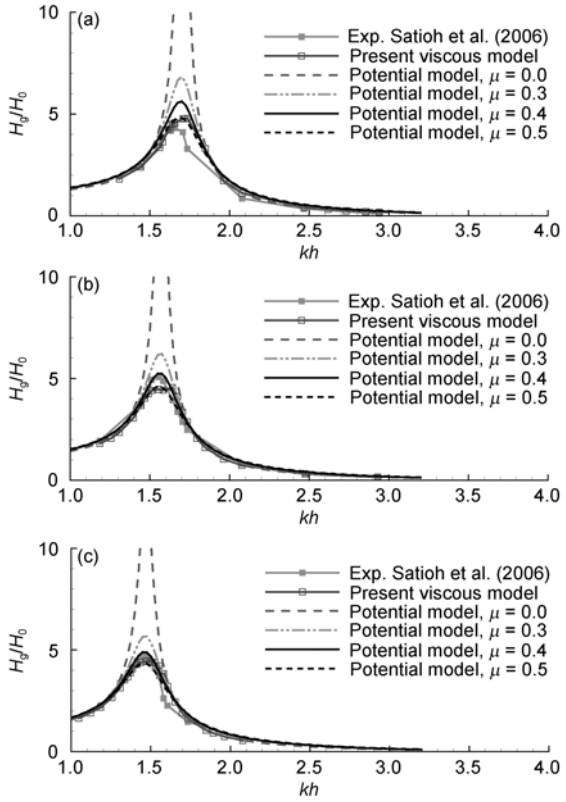


**Figure 2** Comparison of non-dimensional wave height $H_g/H_0$ with respect to incident wave frequency $kh$ for twin boxes at different gap width $B_g$ with the same $D$ = 0.252 m, $B$ = 0.5 m, $h$ = 0.5 m and $H_0$ = 0.024 m. (a) Gap width $B_g$ = 0.03 m ($B_g/B$ = 0.06); (b) gap width $B_g$ = 0.05 m ($B_g/B$ = 0.10); (c) gap width $B_g$ = 0.07 m ($B_g/B$ = 0.14).

shows that, for example the case of Figure 2(b) conducted on a computer with the Intel I7 CPU and 4 G memory, the potential flow model took only about 90 min for the total 69 wave frequencies involved, while the viscous fluid model requires more than 48 hours to simulate the physical process of 60 s at the resonant wave frequency. Therefore, the resonant frequency and the resonant wave height associated with the viscous fluid model in this work are generally referring to the values with acceptable tolerance compared to the experimental observations. In contrast to the good performance of the viscous fluid model, the conventional potential flow model (that is, $\mu$ = 0.0) over-predicts significantly the wave height in narrow gap at the frequencies near the resonant frequency. However, the accuracy of the resonant wave heights based on the potential flow model is improved substantially when a non-zero damping coefficient is used. It can be found from Figure 2 that the wave heights at the resonant frequencies decrease with the increase of damping coefficient. The potential flow model results obtained with $\mu$ = 0.4 and 0.5 appear to agree generally well with the experimental data and the viscous fluid model. It is also observed that the predicted wave heights from the potential flow model are hardly affected by the values of damping coefficient at the frequencies outside a certain band at either side of the resonant frequency.

In order to demonstrate clearly the influence of the gap width, the resonant frequencies and resonant wave heights obtained by laboratory tests and numerical models at various gap widths are summarized in Table 1. It can be seen that the numerical results and experimental investigations indicate coincidently that the resonant frequency tends to decrease with the increase of gap width ($B_g/B$ from 0.06 to 0.14). According to the experimental data, the maximal resonant wave height happens at $B_g$ = 0.05 m. It is speculated that the fluid resistance in the narrow gap may be proportional to the mean vertical velocity gradient in the narrow gap, which can be roughly evaluated by the formula of $\mathrm{d}V/\mathrm{d}x \approx V/B_g$. That is the reason why the measured resonant wave height at $B_g$ = 0.03 m is smaller than that at $B_g$ = 0.05 m, accounted by the increase of $V/B_g$ mainly due to the reduced gap width. On the other hand, the fluid resistance is also affected by the local mean flow velocity, in other words, the actual oscillating amplitude of fluid resonance. As the resonant wave height (velocity) exceeds a critical value, for example the situation of $B_g$ = 0.05 m, it will lead to the absolute increasing of fluid resistance in narrow gaps regardless of the increase of gap width. That means the increase of mean vertical velocity plays the more important role contrasted to the gap width. Hence, we find that the resonant wave height at $B_g$ = 0.07 m is smaller than that observed at $B_g$ = 0.05 m. As for the viscous numerical results, the predicted resonant wave height at $B_g$ = 0.03 m is greater than the experimental data, while the smaller values are produced at $B_g$ = 0.05 m and $B_g$ = 0.07 m. However, the maximal relative difference appearing at $B_g$ = 0.05 m is about 10%, which is acceptably rather small compared to the results of the conventional potential flow model. In addition, the numerical results from the potential flow model with $\mu$ = 0.4 and 0.5 are observed to agree with the experimental data in general with the largest relative errors about 20% and 10%, respectively.

The comparisons shown in Figure 2 and Table 1 appear to suggest that the potential flow model can be used to predict the wave height in the narrow gap if a well calibrated damping coefficient is adopted. However it has to be vali-

**Table 1** Influence of gap width on the resonant frequency and resonant wave height in narrow gap

| Gap width $B_g$ ($B_g/B$) | | 0.03 m (0.06) | 0.05 m (0.10) | 0.07 m (0.14) |
|---|---|---|---|---|
| $kh$ | Experiment [5] | 1.639 | 1.556 | 1.469 |
| | Viscous model | 1.735 | 1.643 | 1.494 |
| | Potential model, $\mu$ = 0.4 | 1.700 | 1.550 | 1.450 |
| | Potential model, $\mu$ = 0.5 | 1.700 | 1.550 | 1.450 |
| $H_g/H_0$ | Experiment [5] | 4.512 | 5.060 | 4.672 |
| | Viscous model | 4.790 | 4.556 | 4.450 |
| | Potential model, $\mu$ = 0.4 | 5.616 | 5.238 | 4.886 |
| | Potential model, $\mu$ = 0.5 | 4.822 | 4.597 | 4.346 |

dated furthermore over a wide range of structural configurations.

### 2.2 Influence of draft

Now we focus on the influence of draft with the fixed gap width of 0.05 m, box breadths of 0.5 m and water depth of 0.5 m. Also, three different drafts, namely $D$ = 0.103 m, 0.153 m and 0.252 m, are considered, which leads to the dimensionless drafts $D/h$ of 0.21, 0.31 and 0.50, respectively. Figures 3(a) and 3(b) show the variation of dimensionless wave height $H_g/H_0$ with incident wave frequency $kh$ at $D$ = 0.103 m and 0.153 m, respectively. As for the case of $D$ = 0.252 m with the same $B_g$ = 0.05 m, $B$ = 0.5 m and $h$ = 0.5 m refers to Figure 2(b).

The numerical results shown in Figures 3(a), 3(b) and 2(b) confirm again that both of the potential flow model and the viscous fluid model are able to predict the resonant frequencies well, despite different drafts are considered in these figures. As far as the variation of $H_g/H_0$ with $kh$ is concerned, the viscous fluid model can produce satisfying results compared to the experimental measurements. On the other hand, the conventional potential model fails to predict the resonant wave heights reasonably, giving rise to unphysical results of more than 10 times of the incident wave height. But it simulates successfully the wave heights in narrow gaps at lower frequencies and higher frequencies.

Similar to the previous examples, as a proper amount of artificial damping is adopted in the potential flow model it can work even as well as the viscous fluid model in predicting the resonant wave height. Generally, the larger damping force is introduced, the smaller resonant wave height is obtained. It seems that the usage of $\mu$ = 0.5 may lead to satisfying results of resonant wave height for the present two cases considered in Figure 3. In addition, it is also interesting to find that the predicted wave heights in narrow gaps are not sensitive to the damping coefficient when the incident wave frequencies are far from the resonant frequency.

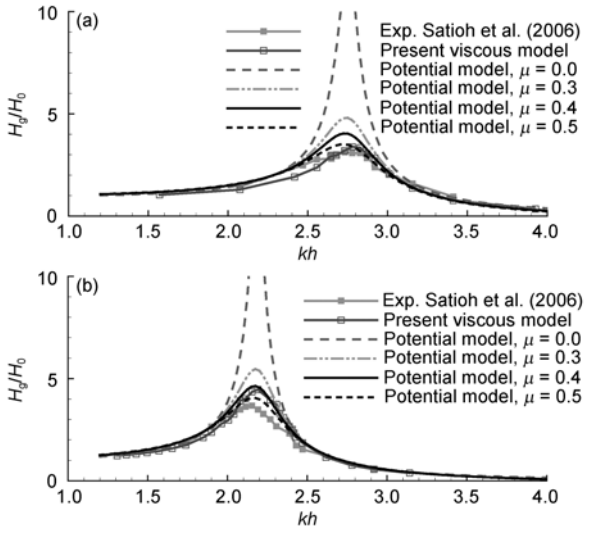


**Figure 3** Comparison of non-dimensional wave height $H_g/H_0$ with respect to incident wave frequency $kh$ for twin boxes at different draft with the same $B$ = 0.5 m, $B_g$ = 0.05 m, $h$ = 0.5 m and $H_0$ = 0.024 m. (a) Draft $D$ = 0.103 m ($D/h$ = 0.206); (b) draft $D$ = 0.153 m ($D/h$ = 0.306).

Comparisons of Figures 3(a), 3(b) and 2(b) show also that the frequency region associated with the fluid resonance becomes broader as the draft decreases gradually. It means that the variation of $H_g/H_0$ with $kh$ is not as sharp as that observed in larger drafts. As for the detailed influence of body draft on the resonant frequency and resonant wave height, the representative quantities are listed in Table 2. It was identified that the resonant frequency decreases substantially with the increase of draft (from 0.103 m to 0.252 m). Actually, it is not surprising to observe this phenomenon since the larger draft can lead to the increase of fluid mass in the narrow gap and consequently the natural frequency of fluid bulk in the narrow gap decreases. According to the experimental data and numerical results obtained in this work, the resonant wave heights in narrow gap trend to increase with the draft. This is mainly induced by the wave conditions under the fluid resonance. It has been confirmed before that the fluid resonance happens at higher frequency as the draft decreases. That means the corresponding fluid resonance in narrow gap will be excited by the short waves and the strong wave reflection might be expected. Therefore, the available wave energy accounted for the fluid resonance in narrow gap decrease. Accordingly, the dimensionless $H_g/H_0$ under small draft is reduced. It should be noted that, on the other hand, the larger draft may increase the total fluid resistance in narrow gap and trend to decrease the resonant wave height because of the increase of wall area exposed to water oscillation in the narrow gap. However, this effect is expected to be limited compared to the previously mentioned wave reflection.

The comparisons of resonant wave height in Table 2 show that the viscous fluid model can produce very good solutions except the case of $D$ = 0.153 m. Looking at the corresponding results shown in Figure 3(b), it seems that the experimental data may involve some measurement errors because the resonant frequency is obviously smaller than

**Table 2** Influence of body draft on the resonant frequency and wave height in narrow gap

| | Draft $D$ ($D/h$) | 0.103 m (0.21) | 0.153 m (0.31) | 0.252 m (0.50) |
|---|---|---|---|---|
| $kh$ | Experiment [5] | 2.732 | 2.154 | 1.469 |
| | Viscous model | 2.778 | 2.191 | 1.494 |
| | Potential model $\mu$ = 0.4 | 2.725 | 2.175 | 1.450 |
| | Potential model $\mu$ = 0.5 | 2.725 | 2.175 | 1.450 |
| $H_g/H_0$ | Experiment [5] | 3.130 | 3.668 | 4.672 |
| | Viscous model | 3.396 | 4.457 | 4.450 |
| | Potential model $\mu$ = 0.4 | 4.043 | 4.626 | 4.886 |
| | Potential model $\mu$ = 0.5 | 3.516 | 4.048 | 4.346 |

the numerical results obtained form both the viscous fluid model and the potential flow model. In contrast to the conventional potential flow model, acceptable predicted resonant wave heights are obtained by introducing artificial damping force. It is identified again that $\mu = 0.4$ and 0.5 can produce satisfying resonant wave height in narrow gap. Compared to the averaging resonant wave heights from the experimental data and the viscous fluid model, the maximal relative errors for $\mu = 0.4$ and 0.5 are around 20% and 10%, respectively. It indicates that $\mu = 0.5$ is also a desirable choice for the present situation involving different drafts, which is in good agreement with the previous findings considering various gap widths.

### 2.3 Influence of individual breadth

In practical applications, two approximating ships are commonly with different cross-section dimensions. Hence it is necessary to investigate the influence from the individual breadths of two boxes in order to propose a reasonable damping coefficient for the potential theory based on the numerical modelling. This is achieved in this work by using the same benchmark of twin boxes with identical draft of 0.252 m, gap width 0.05 m and water depth 0.5 m as considered in Figure 2(b), but reduces the breadth of Body B from 0.5 m to 0.3 m and 0.2 m, respectively, while keeps the breadth of Body A to be the fixed 0.5 m. Therefore, three body breadth ratios of $B_B/B_A$, 1.0, 0.6 and 0.4, are considered in this work. The same as the previous discussions, the variation of $H_g/H_0$ with $kh$ is examined, as shown in Figures 4(a) and 4(b). Also, the special case of $B_B = B_A = 0.5$ m at the same water depth, draft and gap width is referred to Figure 2(b). Note that, Figure 4 presents only the comparison between the results of our viscous numerical model and the potential flow model because the experimental data are not available in the literature. Consequently, the calibration for the damping coefficient of potential flow model is based on the numerical results of the viscous fluid model, since we have shown the excellent performance of the viscous model in simulating the violent fluid oscillation in narrow gap under water waves.

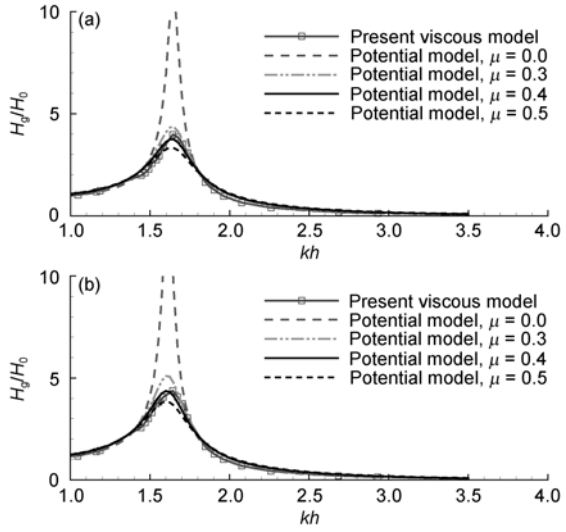


**Figure 4** Comparison of non-dimensional wave height $H_g/H_0$ with respect to incident wave frequency $kh$ at different individual breadths for two boxes with the same $B_g = 0.05$ m, $D = 0.252$ m, $h = 0.5$ m and $H_0 = 0.024$ m. (a) $B_B = 0.2$ m ($B_B/B_A = 0.4$); (b) $B_B = 0.3$ m ($B_B/B_A = 0.6$).

It can be seen from Figures 4(a) and 4(b) that the potential flow model predicts very close resonant frequencies to those obtained from the viscous fluid model. In addition to the frequencies around the fluid resonance, the potential flow models with and without damping force work fairly well, giving rise to satisfying predictions on the amplitude of fluid oscillation in narrow gap. However, the resonant wave heights are also over-predicted by the conventional potential model but can be reduced reasonably by using appropriate artificial damping term.

Careful observations on Figures 4(a), 4(b) and 2(b) indicate that the resonant frequency generally decreases with the increase of the breadth of Body B. That means the resonant frequency is not only dependent on the fluid mass in narrow gap as discussed before but also correlated to the fluid bulk under the floating bodies. The tendency of resonant frequency with respect to the body breadth is in good accordance with the previous theoretical analysis in refs. [5,6].

The numerical results from the viscous fluid model show that the resonant wave height is reduced by decreasing the breadth of Body B located downstream, as shown in Table 3. This can be interpreted by the energy conservation. It is rational to assume that the incident wave energy is nearly identical to the cases considered here since a uniform incident wave height is employed. One may argue that the actual incident wave energy can be affected by the wave reflection and transmission as described in the previous section associated with the body draft. It is true that the resonant wave frequency increases with the decrease of the body breadth $B_B$ and leads to the appearance of fluid resonance under short waves. That means the wave reflection may get stronger. Apparently, the actual incident wave may decrease accordingly. However, for short waves the transmission of wave energy can also become weaker. Hence the collaborated effects from the wave length change are expected to counteract each other. In addition, it can be seen from this table that the change of resonant wave frequency due to breadth is rather limited, resulting in the variation of wave length about 0.2 m, which is believed not to significantly affect the actual incident wave energy. Bearing the above recognitions in mind and considering that much more wave energy can be transmitted to the rear region of the floating bodies due to the decrease of the breadth of Body B, it can be deduced that the wave energy used to support the resonant wave oscillation in narrow gap decreases consequently. Therefore, the resonant wave height is observed to

**Table 3** Influence of individual body breadth on the resonant frequency and wave height in narrow gap

| | Breadth of Body B $B_B$ ($B_B/B_A$) | 0.2 m (0.4) | 0.3 m (0.6) | 0.5 m (1.0) |
|---|---|---|---|---|
| *kh* | Experiment [5] | – | – | 1.469 |
| | Viscous model | 1.643 | 1.640 | 1.494 |
| | Potential model $\mu = 0.4$ | 1.625 | 1.600 | 1.450 |
| | Potential model $\mu = 0.5$ | 1.625 | 1.600 | 1.450 |
| $H_g/H_0$ | Experiment [5] | – | – | 4.672 |
| | Viscous model | 3.975 | 4.366 | 4.450 |
| | Potential model $\mu = 0.4$ | 3.740 | 4.356 | 4.886 |
| | Potential model $\mu = 0.5$ | 3.332 | 3.843 | 4.346 |

decrease in narrow gap with the decrease of box breadth located downstream.

Comparing the numerical results of resonant wave heights obtained by the potential flow model with the damping coefficients of 0.4 and 0.5 with the viscous fluid model and the experimental data (for only the case of $B_B/B_A$ = 1.0), it can be seen that the value of $\mu$ = 0.4 is more desirable with the maximal relative error of 6% while the maximal relative error is 16% at $\mu$ = 0.5. The optimal calibration of $\mu$ = 0.4 is somewhat smaller than the previous tuned value $\mu$ = 0.5. But no substantial difference is observed between the predicted resonant wave heights obtained from $\mu = 0.4$ and $\mu = 0.5$.

### 2.4 Influence of the number of boxes

The fluid resonance in two narrow gaps between three identical fixed boxes was also investigated in this work. This was conducted by intruding an additional Body C behind Body B and leaving the same small separation of 0.05 m between them. The dimensions of water depth $h$ = 0.5 m, draft $D$ = 0.252 m, breadth of the boxes $B$ = 0.5 m are set to be identical to those used in the previous cases of twin bodies with a single narrow gap. The gap between Body A and Body B is referred to as Gap 1 herein and that between Body B and Body C is defined as Gap 2. By using a uniform incident wave height of $H_0$ = 0.024 m under various *kh*, the numerical results of $H_g/H_0$ in Gap 1 and Gap 2 from the viscous fluid model and potential flow model are compared with the experimental data [6], as shown in Figures 5(a) and 5(b).

It can be seen from Figure 5(a) that the variation of $H_g/H_0$ with *kh* in Gap 1 from viscous flow model agrees well with the experimental data in general but with a small phage lag. Both the viscous flow model results and the experimental data show that the variation of wave height in Gap 1 has two peak values. This suggests that the fluid resonance in Gap 1 takes place at two distinct frequencies in contrast to the single resonant frequency in the case of twin bodies with one narrow gap. The double-peak variation of $H_g/H_0$ with *kh* is also observed in Gap 2, as shown in Figure

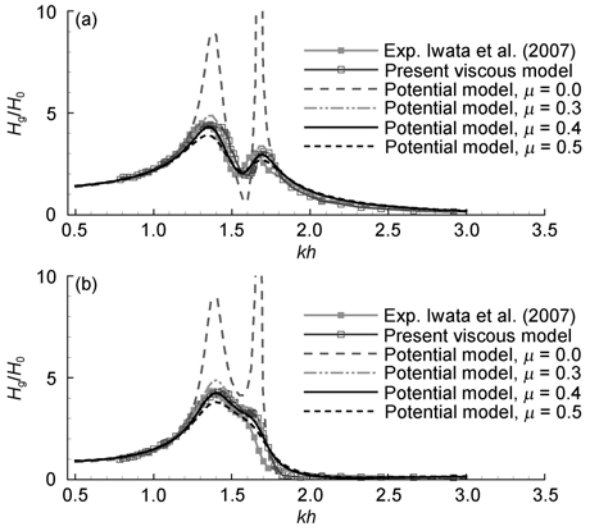


**Figure 5** Comparison of non-dimensional wave height $H_g/H_0$ with respect to incident wave frequency *kh* in two narrow gaps between three identical boxes, (a) for Gap 1 and (b) for Gap 2, at $B_g$ = 0.05 m, $D$ = 0.252 m, $B$ = 0.5m, $h$ = 0.5 m and $H_0$ = 0.024 m.

5(b), although the second resonant response is not as significant as that in Gap 1. The existence of two resonant frequencies is mainly attributed to the presence of the second narrow gap or the intrusion of the third box.

Obvious discrepancies between the results of the conventional potential flow model ($\mu$ = 0.0) and laboratory tests can be observed in Figures 5(a) and 5(b) over the bands around the resonant frequencies. At the first resonant frequency, $H_g/H_0 \approx 10$ is predicted by the conventional potential flow model, which is more than two times of the results of the viscous flow model and the model tests. At the second resonant frequency, the conventional potential flow model predicts $H_g/H_0 > 30$, which is more than 7.5 times of the values obtained from physical model tests [6]. However, as for the frequencies far away from the resonant band, the predicted wave heights based on the potential flow model have little dependence on the values of the damping coefficient. This is similar to what was observed in the previous cases involving twin bodies with different gap widths, drafts and breadth ratios. It was observed again that the wave heights in narrow gaps around the fluid resonant frequencies decrease with the increase of the damping coefficient. It is found that the value of $\mu$ = 0.4 leads to relatively accurate predictions of the resonant wave heights. It is worth noting that the specific value of $\mu = 0.4$ is valid not only for Gap 1 but also for Gap 2.

The comparisons of results shown in Figures 5(a) and 5(b) indicate that the phase-lag between the experimental data and potential flow model results also exist, similar to the results from the viscous fluid model. Actually, the variation of $H_g/H_0$ versus *kh* from the potential flow model with artificial damping forces agrees much better with the results of the viscous fluid model.

Following the previous procedure, we firstly demonstrate the comparisons in quantity on the results in Gap 1 of three bodies with the case of two bodies. It can be seen from Table 4 that the fundamental resonant frequency in Gap 1 is smaller than that observed in the case of twin bodies, while the second resonant frequency is greater than the resonant frequency of twin boxes. It seems that the resonant frequencies observed in experiments are slightly smaller than those obtained by numerical predictions using both the viscous fluid model and the potential flow model. As for the resonant wave heights in Gap 1 of three bodies, they are observed to be smaller than that of twin bodies, both at the first frequency and the second frequency. It appears that the potential model with $\mu = 0.4$ can produce better solutions of the resonant wave heights in Gap 1 at both distinct resonant frequencies. The comparisons of resonant frequencies and resonant wave heights in Gap 2 are presented in Table 5. Since the second resonant frequency from experimental measurement and the viscous fluid model are not as obvious as that observed in Gap 1, the roughly estimated values are provided in Table 5. For the numerical results of the potential flow model with damping term, they are determined alternatively using the results based on the conventional potential flow model. Similar to the previously described results associated with Gap 1, the resonant frequency of twin bodies is found to be between the first and second resonant frequencies of three bodies. Two smaller resonant wave heights are also observed in the case of three bodies with respect to that of twin bodies with single narrow gap. It means that the resonant wave heights are reduced by increasing the box number regardless of how many resonant frequencies in presence. In addition, the appropriate damping coefficient $\mu = 0.4$ can also be identified, but gives rise to a slightly larger error contrasted to the results observed in Gap 1.

**Table 4** Influence of body number on the resonant frequency and wave height in Gap 1

| | Number of Bodies | 2 | 3 | |
|---|---|---|---|---|
| | | | 1st Freq. | 2nd Freq. |
| $kh$ | Experiment [6] | 1.469 | 1.307 | 1.640 |
| | Viscous model | 1.494 | 1.334 | 1.702 |
| | Potential model, $\mu = 0.4$ | 1.450 | 1.350 | 1.700 |
| | Potential model, $\mu = 0.5$ | 1.450 | 1.350 | 1.700 |
| $H_g/H_0$ | Experiment [6] | 4.672 | 4.484 | 3.026 |
| | Viscous model | 4.450 | 4.383 | 3.081 |
| | Potential model, $\mu = 0.4$ | 4.886 | 4.318 | 2.948 |
| | Potential model, $\mu = 0.5$ | 4.346 | 3.905 | 2.680 |

**Table 5** Influence of body number on the resonant frequency and wave height in Gap 2[a)]

| | Number of Bodies | 2 | 3 | |
|---|---|---|---|---|
| | | | 1st Freq. | 2nd Freq. |
| $kh$ | Experiment [6] | 1.469 | 1.374 | 1.586* |
| | Viscous model | 1.494 | 1.438 | 1.626* |
| | Potential model, $\mu = 0.4$ | 1.450 | 1.400 | 1.675+ |
| | Potential model, $\mu = 0.5$ | 1.450 | 1.400 | 1.675+ |
| $H_g/H_0$ | Experiment [6] | 4.672 | 4.333 | 2.981 |
| | Viscous model | 4.450 | 4.313 | 3.292 |
| | Potential model, $\mu = 0.4$ | 4.886 | 4.254 | 2.495 |
| | Potential model, $\mu = 0.5$ | 4.346 | 3.794 | 2.232 |

a) Note, * roughly estimated; + determined by potential flow model with $\mu = 0.0$.

## 3 Concluding remarks

Numerical simulations of fluid resonance in narrow gaps under water waves are conducted in this work employing both the viscous fluid model and the potential flow model with and without artificial damping force.

Based on the comprehensive numerical results of the viscous fluid model and available experimental data, the influences of gap width, body draft, breadth ratio and body number on the resonant frequency and resonant wave height in narrow gaps were investigated. The main findings include:

(1) With the increase of gap width, the resonant frequency moves towards lower frequency. However, the maximal resonant wave height appears at a particular gap width, determined by the counter effects from mean velocity in the narrow gap and gap width.

(2) Increasing the body draft, the resonant frequency is observed to shift towards the lower region. Meanwhile, the resonant wave height tends to increase for the cases considered in this work.

(3) When the breadth of downstream body is reduced, the resonant frequency increases while the resonant height decreases.

(4) By introducing an identical floating body to the assembly, two distinct resonant frequencies are observed. The fundamental frequency is smaller than the resonant frequency of twin bodies, while the second frequency is higher than the resonant frequency of twin bodies. The resonant wave heights of three bodies are generally smaller than that observed for twin bodies. In addition, the resonant wave height under fundamental frequency is found to be greater than that associated with the second resonant frequency in the both gaps.

The numerical results from the conventional potential flow model show that it is able to capture the resonant frequency as accurately as the laboratory tests and the viscous fluid model. However, it fails to predict the resonant wave height in narrow gaps, generally giving rise to much more over-prediction.

By introducing appropriate damping force into the potential flow model, the accuracy of the predicted resonant wave height in narrow gaps can be improved greatly. It was conformed in this work that when $\mu \in [0.4, 0.5]$ is adopted, the

potential flow model is capable of predicting the resonant wave height in narrow gaps as well as the experimental tests and the viscous fluid model, while the computational efforts can be saved greatly. It is promising that the calibrated damping coefficient is observed not sensitive to the variation of gap width, body draft, body number and individual breadth ratio according to the verifications conducted in this work. The maximal relative error is limited within 20% for the different body configurations and arrangements considered in this work.

*The first author gratefully acknowledges the financial supports from the Natural National Science Foundation of China (Grant Nos. 50909016, 50921001 and 10802014). Part of the present work was conducted while the first author was visiting the University of Western Australia with the support of ARC Discovery Project Program (Grant No. DP0557060). This work was also partially supported by the Open Fund from the State Key Laboratory of Structural Analysis for Industrial Equipment (Grant No. GZ0909).*

1 Kagemoto H, Yue D K P. Hydrodynamic interaction analysis of very large floating structures. Mar Struct, 1993, 6: 295–322
2 Koo B J, Kim M H. Hydrodynamic interactions and relative motions of two floating platforms with mooring lines in side-by-side offloading operation. Appl Ocean Res, 2005, 27: 292–310
3 Kristiansen T, Faltinsen O M. A two-dimensional numerical and experimental study of resonant coupled ship and piston-mode motion. Appl Ocean Res, 2010, 32: 158–176
4 Kristiansen T, Faltinsen O M. Studies on resonant water motion between a ship and a fixed terminal in shallow water. J Offshore Mech Arct Eng, 2009, 131: 021102
5 Saitoh T, Miao G P, Ishida H. Theoretical analysis on appearance condition of fluid resonance in a narrow gap between two modules of very large floating structure. In: Proceedings of the 3rd Asia-Pacific Workshop on Marine Hydrodynamics. Beijing: China Ocean Press, 2006. 170–175
6 Iwata H, Saitoh T, Miao G P. Fluid resonance in narrow gaps of very large floating structure composed of rectangular modules. In: Proceedings of the 4th International Conference on Asian and Pacific Coasts. Beijing: China Ocean Press, 2007. 815–826
7 Miao G P, Ishida H, Saitoh T. Influence of gaps between multiple floating bodies on wave forces. China Ocean Eng, 2000, 14: 407–422
8 McIver P. Complex resonances in the water-wave problem for a floating structure. J Fluid Mech, 2005, 536: 423–443
9 Miao G P, Saitoh T, Ishida H. Water wave interaction of twin large scale caissons with a small gap between. Coast Eng J, 2001, 43: 39–58
10 Li B N, Cheng L, Deeks A J, et al. A modified scaled boundary finite element method for problems with parallel side-faces. Part II. Application and evaluation. Appl Ocean Res, 2005, 27: 224–234
11 Fitzgerald C J, McIver P. Approximation of near-resonant wave motion using a damped harmonic oscillator model. Appl Ocean Res, 2009, 31: 171–178
12 Teng B, He G H, Li B N, et al. Research on the hydrodynamic influence from the gap between twin caissons by a scaled boundary finite element method (in Chinese). The Ocean Eng, 2006, 24: 29–37
13 He G H, Teng B, Li B N, et al. Research on the hydrodynamic influence from the gaps between three identical boxes by a scaled boundary finite element method (in Chinese). J Hydrodyn Ser A, 2006, 21: 418–424
14 Molin B. On the piston and sloshing modes in moonpools. J Fluid Mech, 2001, 430: 27–50
15 Faltinsen O M, Rognebakke O F, Timokha A N. Two-dimensional resonant piston-like sloshing in a moonpool. J Fluid Mech, 2007, 575: 359–397
16 Sun L, Eatock Taylor R, Taylor P H. First and second-order analysis of resonant waves between adjacent barges. J Fluids Struct, 2010, 26: 954–978
17 Zhu R C, Miao G P, You Y X. Influence of gaps between 3-D multiple floating structures on wave forces. J Hydrodyn Ser B, 2005, 17: 141–147
18 Zhu H R, Zhu R C, Miao G P. A time domain investigation on the hydrodynamic resonance phenomena of 3-D multiple floating structures. J Hydrodyn, 2008, 20: 611–616
19 Huijsmans R H M, Pinkster J A, Wilde J J. Diffraction and radiation of waves around side by side moored vessels. In: Proceedings of the 11th International Offshore and Polar Engineering Conference. Cupertino: ISOPE, 2001. 406–412
20 Newman J N. Progress in wave load computations on offshore structures. In: Proceedings of the 23th Conference on Offshore Mechanics and Arctic Engineering. New York: ASME, 2004. Invited Lecture
21 Chen X B. Hydrodynamics in Offshore and Naval Applications. In: Proceedings of the 6th International Conference on Hydrodynamics —Part I. Keynote lecture of the 6th International Conference on Hydrodynamics. London: Taylor & Francis Group, 2004
22 Pauw W H, Huijsmans R, Voogt A. Advances in the hydrodynamics of side-by-side moored vessels. In: Proceedings of the 26th Conference on Offshore Mechanics and Arctic Engineering. New York: ASME, 2007. 29374
23 Bunnik T, Pauw W, Voogt A. Hydrodynamic analysis for side-by-side offloading. In: Proceedings of the 19th International Offshore and Polar Engineering Conference. Cupertino: ISOPE, 2009. 648–653
24 Lu L. Investigation of fluid resonance in narrow gaps between marine structures based on viscous numerical wave flume. Post-doc Report. Dalian: Dalian University of Technology, 2008. 1–69
25 Lu L, Cheng L, Teng B, et al. Numerical simulation of hydrodynamic resonance in a narrow gap between twin bodies subject to water waves. In: Proceedings of the 18th International Offshore and Polar Engineering Conference. Cupertino: ISOPE, 2008. 114–119
26 Lu L, Cheng L, Teng B, et al. Numerical investigation of fluid resonance in two narrow gaps of three identical rectangular structures. Appl Ocean Res, 2010, 32: 177–190
27 Jiang C B, Kawahara M. The analysis of unsteady incompressible flows by a 3-step finite-element method. Int J Numer Methods Fluids, 1993, 16: 793–811
28 Lin P Z, Liu P L F. Internal wave maker for Navier-Stokes equations models. J Waterw Port Coastal Ocean Eng, 1999, 125: 207–215
29 Ashgriz N, Barbat T, Wang G. A computational Lagrangian-Eulerian advection remap for free surface flows. Int J Numer Methods Fluids, 2004, 44: 1–32
30 Kim M H, Niedzwechi J M, Roesset J M, et al. Fully nonlinear multidirectional waves by a 3-D viscous numerical wave tank. J Offshore Mech Arct Eng, 2001, 123: 124–133
31 Li Y C, Chen B, Lai G Z. Numerical simulation of wave forces on seabed pipelines. China Ocean Eng, 1998, 12: 203–211
32 Van der Vorst H A. BI-CGSTAB: A fast and smoothly converging variant of BI-CG for the solution of nonsymmetric linear-system. SIAM J Sci Stat Comput, 1992, 13: 631–644
33 Yang C, Löhner R, Lu H D. An unstructured-grid based volume-of-fluid method for extreme wave and freely-floating structure interactions. J Hydrodyn Ser B, 2006, 18: 415–422
34 Löhner R, Yang C, Oñate E. Simulation of flows with violent free surface motion and moving objects using unstructured grids. Int J Numer Methods Fluids, 2007, 53: 1315–1338
35 Li Y C, Teng B. Wave Action on Maritime Structures. 2nd ed. Beijing: Marine Press, 2002